

# Genomic scale profiling of nutrient and trace elements in *Arabidopsis thaliana*

Brett Lahner<sup>1</sup>, Jiming Gong<sup>2</sup>, Mehrzad Mahmoudian<sup>1</sup>, Ellen L Smith<sup>1</sup>, Khush B Abid<sup>2</sup>, Elizabeth E Rogers<sup>3</sup>, Mary L Guerinet<sup>4</sup>, Jeffrey F Harper<sup>5</sup>, John M Ward<sup>6</sup>, Lauren McIntyre<sup>7</sup>, Julian I Schroeder<sup>2</sup> & David E Salt<sup>1</sup>

Understanding the functional connections between genes, proteins, metabolites and mineral ions is one of biology's greatest challenges in the postgenomic era. We describe here the use of mineral nutrient and trace element profiling as a tool to determine the biological significance of connections between a plant's genome and its elemental profile. Using inductively coupled plasma spectroscopy, we quantified 18 elements, including essential macro- and micronutrients and various nonessential elements, in shoots of 6,000 mutagenized M2 *Arabidopsis thaliana* plants. We isolated 51 mutants with altered elemental profiles. One mutant contains a deletion in *FRD3*, a gene known to control iron-deficiency responses in *A. thaliana*. Based on the frequency of elemental profile mutations, we estimate 2–4% of the *A. thaliana* genome is involved in regulating the plant's nutrient and trace element content. These results demonstrate the utility of elemental profiling as a useful functional genomics tool.

The plant biology community aims to establish the biological function of all genes in the *A. thaliana* genome (refs. 1,2). To achieve this, generation of both transgenic and mutant plants has been coupled to large-scale analysis of gene products such as mRNA<sup>3,4</sup>, proteins<sup>5,6</sup> and cellular metabolites<sup>7,8</sup>. Such functional genomics approaches allow the links between genes and the organic chemistry of living systems to be established. However, these approaches do not address how plants control their mineral nutrient and trace element compositions. Here we present a functional genomics approach for gaining insight into gene networks involved in mineral-ion accumulation in plants. Uptake and translocation of mineral ions is essential for plant growth, human health and nutrition, and plant-based bioremediation<sup>9</sup>. Notably, bioremediation and enhanced nutritional value of crops were recently ranked among the top ten biotechnologies for improving human health in developing countries<sup>10</sup>. In spite of recent advances<sup>11</sup>, the gene networks that control acquisition of individual mineral ions remain largely unknown. An understanding of these networks and how they interact with other cellular systems such as the genome, the proteome and the environment are essential to full understanding of how plants integrate their organic and inorganic metabolisms. Here we introduce the term 'ionome' to include all the mineral nutrient and trace elements found in an organism—extending the metallome<sup>12,13</sup> to include metals, metalloids and non-metals. By profiling the mineral ion and trace element compositions of both transgenic and mutant *A. thaliana* plants, we hope to uncover the gene networks that regulate the ionome and its interactions.

Before successful elemental profiling can be achieved, multi-element analysis of plant samples as a rapid, robust, sensitive and precise analytical system needs to be established. Various techniques including flame atomic absorption spectroscopy and inductively coupled plasma spectroscopy (ICP-MS) have been used for both single- and multiple-element analysis of plant samples. To optimize for high-throughput, sensitivity and precision, we chose to use ICP-MS as our primary analytical tool. The high sensitivity and large dynamic range of this instrument allows the precise, simultaneous determination of macro- and micronutrients and trace elements in small tissue samples. This capability allows nondestructive sampling of plants, which is a very useful in a genetic screen. A drawback of the method is that interferences from nitrogen, oxygen and water prevent the quantification of nitrogen and sulfur in plant samples by ICP-MS. We also present data in which the elemental-profiling system has been established to work with inductively coupled plasma atomic emission spectroscopy (ICP-AES).

Here we describe the successful profiling of lithium, sodium, magnesium, phosphorus, potassium, calcium, chromium, manganese, iron, cobalt, nickel, copper, zinc, arsenic, selenium, molybdenum, cadmium and lead in 10,000 M2, M3 and wild-type *A. thaliana* plants by ICP-MS, and of lithium, sodium, magnesium, phosphorus, potassium, calcium, barium, manganese, iron, rubidium, sulfur, zinc and cadmium in 2,500 plants by ICP-AES. This analysis allowed the identification of 51 elemental profile mutants. One of these carries a deletion of 7 base pairs (bp) in *FRD3*, a member of the multidrug and toxin efflux family

<sup>1</sup>Center for Plant Environmental Stress Physiology, Horticulture Building, 625 Agriculture Mall Drive, Purdue University, West Lafayette, Indiana 47907, USA.

<sup>2</sup>Division of Biological Science, Cell and Developmental Biology Section and Center for Molecular Genetics 0116, University of California, San Diego, 9500 Gilman Drive, La Jolla, California 92093, USA. <sup>3</sup>Department of Nutritional Sciences, 217B Gwynn Hall, University of Missouri, Columbia, Missouri 65211, USA.

<sup>4</sup>Department of Biological Sciences, 6044 Gilman, Dartmouth College, Hanover, New Hampshire 03755, USA. <sup>5</sup>The Scripps Research Institute, Department of Cell Biology, Mail Drop BCC283, 10550 North Torrey Pines Road, La Jolla, California 92037, USA. <sup>6</sup>Department of Plant Biology, University of Minnesota, 250 Biological Science Center, 1445 Gortner Avenue, St. Paul, Minnesota 55108, USA. <sup>7</sup>Agricultural Genomics, Department of Agronomy, 915 State Street, Purdue University, West Lafayette, Indiana 47907, USA. Correspondence should be addressed to D.E.S. (dsalt@purdue.edu).

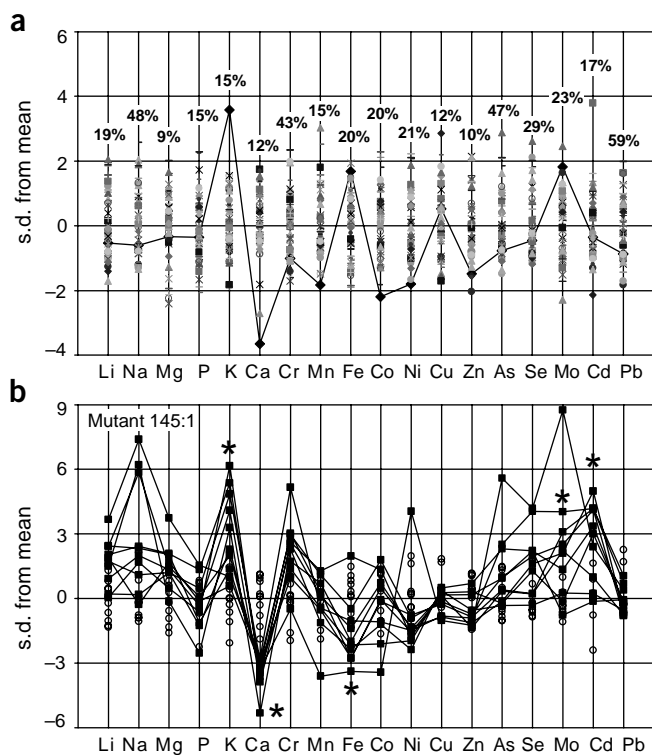


**Figure 1** Mutant identification charts of a selected mutant in M2 and M3 generations. **(a)** Ion-profile data from a complete tray of 60 M2 plants. Mean and standard deviation for each element were calculated for all plants in a tray, excluding the positive-control *frd3-3* plants, and these were used to calculate the number of standard deviations by which each individual plant varied from the whole-tray mean for each element. This data is represented by symbols. Data for mutant 145:1 is highlighted with a solid line, graphically showing this mutant has values over 3 standard deviations high for potassium and low for calcium compared to the whole-tray mean. Numbers on the chart represent the median %RSD for each element calculated using weight-normalized data from all plants within an M2 tray (excluding *frd3-3* plants). The median value represents %RSD values from 54 trays grown over a 4-month period. **(b)** Ion-profile data for mutant 145:1 M3 plants and wild-type plants, from a tray containing plants from five M3 families, wild-type and the *frd3-3* positive control. Means and standard deviations are calculated for each element from wild-type plants ( $n = 11$ ) and used to calculate the number of standard deviations each M3 plant is distant from the mean wild-type value for each element. Data from M3 progeny of mutant 145:1 ( $n = 9$ ) is highlighted with a solid line and wild-type plants with open circles, graphically showing that M3 progeny of mutant 145:1 display higher potassium and lower calcium than wild type. \*, elements for which values from the mutant are significantly different ( $P \leq 0.05$ ) from those from the wild type.

gene known to control iron-deficiency responses in *A. thaliana*<sup>14</sup>. In this proof-of-concept screen, we analyzed approximately 12%<sup>15,16</sup> of the *A. thaliana* genome for mutations affecting elemental accumulation.

## RESULTS

### Identification of mutants with altered elemental profiles

Putative mutants in the M2 generation were identified by plotting all of the elemental profile data from individual trays, containing approximately 70 plants each, using a plotting method related to manufacturing control charts<sup>17</sup>. Control charts are a quality assurance technique commonly used to assess whether the process under consideration is behaving within defined parameters. We have adopted this method

such that the number of s.d. from the whole-tray mean is plotted on the ordinate and each element plotted along the abscissa (Fig. 1a). As expected statistically, at least 95% of the data fall within two s.d. above or below the mean (Fig. 1a). Each tray of M2 plants also contained, as a positive control, up to five *frd3-3* mutants<sup>14</sup>, which are known to have elevated concentrations of several elements, including manganese. In the M2 generation, plants were identified as putative mutants if they contained elements in amounts that were more than 2 s.d. from the mean in either direction (Fig. 1a). Using this criterion, 338 putative mutants were identified from a total collection of 4,747 M2 plants (representing 2,373 M1 parental lines) by ICP-MS. In this method, sensitivity of mutant detection is directly related to the size of the s.d. for a given element. For the majority of elements analyzed by ICP-MS, the s.d. as a percentage of the mean accumulation for each element (percent relative standard deviation, %RSD) was routinely 10–25% (Fig. 1a), allowing detection of mutants in the M2 generation altered by 20–50% (2 s.d.) as compared to the rest of the plants in the tray (Fig. 1a). Putative mutants with alterations in elements quantified with high s.d., including sodium, chromium, arsenic, selenium and lead, were detected with lower sensitivity (Fig. 1a). Extensive analysis of a standardized *A. thaliana* sample shows that on mean analytical variability accounts for approximately 8–22% of the error in values for lithium, zinc, arsenic, selenium, molybdenum, cadmium and lead, 45–68% of the error for phosphorus, calcium, manganese and cobalt, and 100% of the error for magnesium, nickel and copper.

Putative M2 mutants were allowed to self-fertilize and the elemental profiles of the M3 progeny ( $n = 11$ ) were compared to the mean and standard deviation of wild-type plants ( $n = 11$ ) grown in the same tray (Fig. 1b). Of the 338 original M2 putative mutants, 320 produced viable seed. Altered elemental profiles in the M3 putative mutants were assessed using four criteria, including a Student's *t*-test at the 0.05 level of confidence for each element in comparison to that of wild type, a test for differences between the mutant families in each tray (to control for atypical wild-type scores), a visual inspection of the data to check for segregation patterns that would have affected the results of the *t*-tests, and finally a similarity between the elemental profiles in the M2 and M3 generations (Fig. 1a,b). Custom Microsoft Excel tools were developed and used to facilitate this data analysis.

Of the 320 putative mutants rescreened, 44 were confirmed, using these criteria, to have altered elemental profiles as compared to those of wild-type plants, and were termed mutants. Based on this ICP-MS data, approximately 2% of the M1 fast neutron-mutagenized lines screened showed some sort of reproducible disruption in elemental profile. These mutants have many different types of elemental-profile changes, including changes in multiple elements, micronutrients and macronutrients (Figs. 1b and 2). Growth of nine of the most distinct mutants on half-strength Murashige-Skoog (MS) plates followed by ICP-MS analysis of digested shoot material confirmed their mutant phenotypes on defined media. Numerical data for all confirmed mutants are shown in Table 1.

The majority of mutations appear to be homozygous in the M2 population, showing no obvious segregation in the M3 generation. However, using ICP-MS we have identified a single mutant, line 131:36, that segregates for an altered elemental profile in the M3 generation (Fig. 3a). Approximately 25% of the M3 individuals screened showed a substantial increase in both manganese (208%) and cobalt (165%) and decreased iron (–26%) and molybdenum (–41%) when grown in soil (4 in 19) (Fig. 3a) or on half-strength MS plates (3 in 15) (data not shown). Interestingly, the majority of the remaining M3 plants also showed elevated manganese (15%) and cobalt concentrations (12%) ( $P < 0.01$ ), though the magnitude of these differences was much

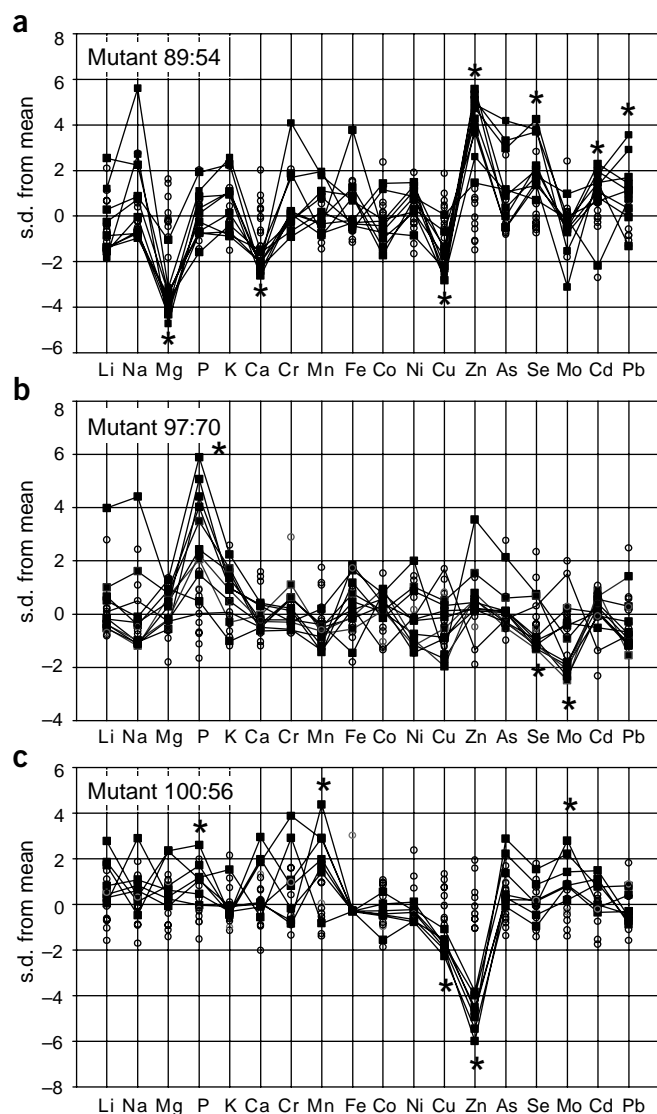


**Figure 2** Mutant identification charts of selected mutant and wild-type plants. Shown are data (analyzed as described in Fig. 1), from the M3 generation of three selected mutants, 89:54 (a), 97:70 (b), and 100:56 (c), respectively. Data for the mutant are shown as a solid line ( $n = 7-11$ ) and wild-type growing in the same tray ( $n = 9-11$ ) shown as open circles. \*, elements for which values from the mutant are significantly different from those from the wild type ( $P \leq 0.05$ ).

reduced. These data suggest that 131:36 is a semidominant mutation, and explains how we were able to identify a heterozygous individual in our M2 screen. The phenotype observed for 131:36 is identical to that of *frd3-3* plants grown under the same conditions (Fig. 3b). Elevated cobalt in *frd3* shoots has not been previously reported, and is intriguing in light of the recent observation that cobalt can regulate the Fe regulon in yeast<sup>18</sup>. Further analysis of this mutant showed that approximately 25% (13 in 60) have constitutively elevated Fe(III) chelate reductase activity (data not shown), a phenotype also shared with *frd3-3*. Progeny from crosses between 131:36 plants with the strong reductase and metal phenotype and homozygous *frd3-2* all showed constitutively elevated Fe(III) chelate reductase activity (data not shown), establishing that 131:36 belongs to the same complementation group as *frd3-3*. Cloning and sequencing from line 131:36 of the *FRD3* gene known to be disrupted in

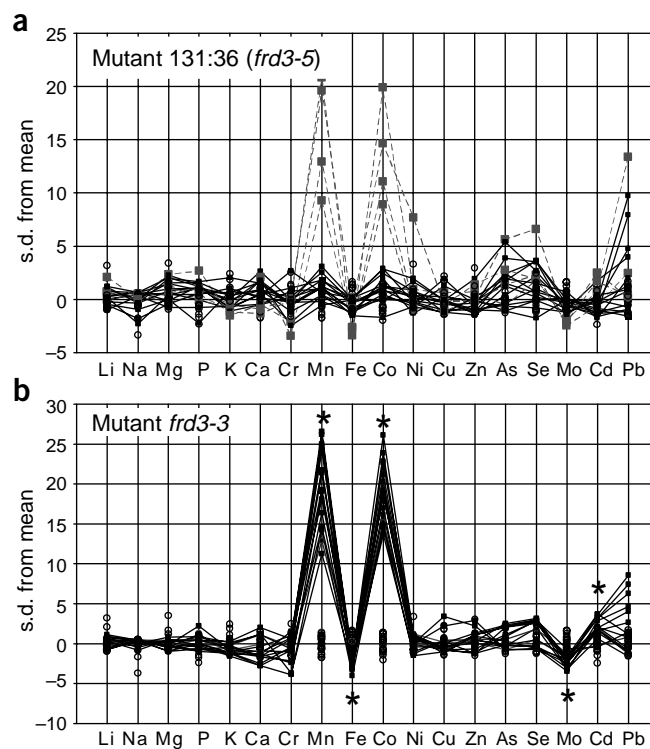


**Figure 3** Mutant identification chart of segregating mutant allele with *frd3*. (a) Data (analyzed as described in Fig. 1), from the M3 generation of mutant 131:36 represented by solid squares and lines. Of the 18 131:36 M3 plants analyzed, 4 had elemental-profiles similar to that of *frd3-3* (highlighted with dashed lines). (b) Data from homozygous *frd3-3* plants ( $n = 19$ ) grown in the same tray as the plants used in a. \*, elements for which values from the mutant are significantly different from those from the wild type ( $P > 0.01$ ), including manganese (259%), cobalt (232%), iron (-27%), molybdenum (-42%) and cadmium (24%). Data in each panel are from one representative tray of two with boron replacing chromium.

*frd3* (ref. 14) revealed a 7-bp deletion in *FRD3* that is 320 bp downstream of the ATG toward the start of a cytoplasmic loop between predicted transmembrane domains two and three. In the predicted translation product of the gene, the first 108 amino acids are the same as those of wild type; the 7-bp deletion causes a frameshift that results in 59 novel amino acids being inserted before a stop codon is encountered. Because the mutation in 131:36 represents a new fifth allele of *frd3* (ref. 14), we have named this mutant *frd3-5*. The semidominance of other *frd3* alleles has not been reported. It is possible that the novel 59 amino acids inserted at the end of *frd3-5* may produce its semidominant negative effect by destabilizing an as-yet-undefined protein complex. Both *frd3-2* and *frd3-3* also produce truncated proteins but with only seven and two novel amino acids added, respectively<sup>14</sup>.

We also carried out experiments using ICP-AES. This technique is generally less sensitive, and has a smaller dynamic range than ICP-MS; however, ICP-AES instruments are generally more available. We established the feasibility of using ICP-AES to perform ion profiling on 13 elements by analyzing ion profiles from 1,191 fast neutron-mutagenized M2 plants. Using ICP-AES, we were able to identify seven mutants using criteria similar to those used in the ICP-MS screen, including *t*-test ( $P \leq 0.05$ ) and similarity between the M2 and M3 elemental profiles. These mutants showed diverse nutrient profiles, including enhanced accumulation of sodium and of the micronutrients manganese and zinc (Table 1).

**Table 1** Statistically significant changes in the elemental profile of mutants compared to wild type

Line	Significant mean percentage change compared to wild type																	
	Li	Na	Mg	P	K	Ca	Cr	Mn	Fe	Co	Ni	Cu	Zn	As	Se	Mo	Cd	Pb
58:54					125													
71:13 <sup>a</sup>			-25			<b>-16</b>										-40		
76:24		-20		-16		-12				-10	-35	-10				36		
79:48			-18						-21							37		
82:70	10	100	16	31			30		30		40		24	100			-10	
86:26																	15	
89:54 <sup>a</sup>			<b>-28</b>			<b>-16</b>						-23	29		30		<b>13</b>	90
91:55																26		
94:62													6					
94:68						-10						-62	-10				22	
96:42									-8	-8							10	
97:70 <sup>a</sup>				<b>28</b>											<b>-26</b>	<b>-52</b>		
98:49 <sup>a</sup>	-15		-10					<b>54</b>								-57		
99:26					28			-10		25								
100:56 <sup>a</sup>				16				<b>20</b>				-60	<b>-42</b>			17		
106:13														350	75		-31	
109:25							80	-22		-19	20						50	
110:35 <sup>a</sup>			<b>20</b>			<b>-31</b>										<b>19</b>		
110:57														222	96			
111:12				32												-35	32	
112:50 <sup>a</sup>			22			<b>-33</b>			-18									
114:38	148			66	147		113	46		172	96			179	150			
116:49				17	-22								13					
117:20	93		93		-24		68							104	60	20		
118:65 <sup>a</sup>			<b>24</b>		47								<b>-23</b>	40	37			
120:01			29			13		40		37								
121:33						-29										34	10	
124:05					-22	-23											39	
131:07																19	-15	
131:36 <sup>a</sup>								<b>208</b>	<b>-26</b>	<b>165</b>							<b>-41</b>	
131:61	21								-17									
132:01	32		53		30	15								112		-40		
132:31						-10			-10			-30						
132:35	14	49			26			-15		-15				95				
132:59								24										
134:19	65	99	30	10	39							-60	-20	250				
135:11	20	69		-15				-22		-26		-30		118			20	
136:31	47		79		121			-36						195	22			
136:32		50			35			-20				-30	-20			20		
145:01 <sup>a</sup>					30	<b>-37</b>			<b>-14</b>							<b>30</b>	<b>18</b>	
145:38					-12				-14				-15		-40		10	
152:19	10							-14								20		
152:54			-9	10		-9		20										
162:29	-31		-17				-9								-21			
180 <sup>b</sup>					-27								147				-53	
282 <sup>b</sup>		469																
380 <sup>b</sup>													115					
492 <sup>b</sup>								130					86					
591 <sup>b</sup>								100										
781 <sup>b</sup>													157					
1148 <sup>a,b</sup>		<b>972</b>																

<sup>a</sup>Mutant phenotype confirmed on half-strength MS plates. <sup>b</sup>Mutants identified using ICP-AES. Data represents the mean percentage change in concentration of elements that were statistically significantly different in the mutant as compared to the wild type ( $P \leq 0.05$ ,  $n = 8-11$ ). Numbers in bold italics represent changes in soil-grown plants that were also observed to be significant ( $P \leq 0.05$ ,  $n = 8-20$ ) when mutant lines were grown on Petri dishes containing 0.8% agar and half-strength MS basal salt with Gamborg's vitamins. Potassium selenate (0.1  $\mu\text{M}$ ) was also added to the MS medium for line 97:70 only.

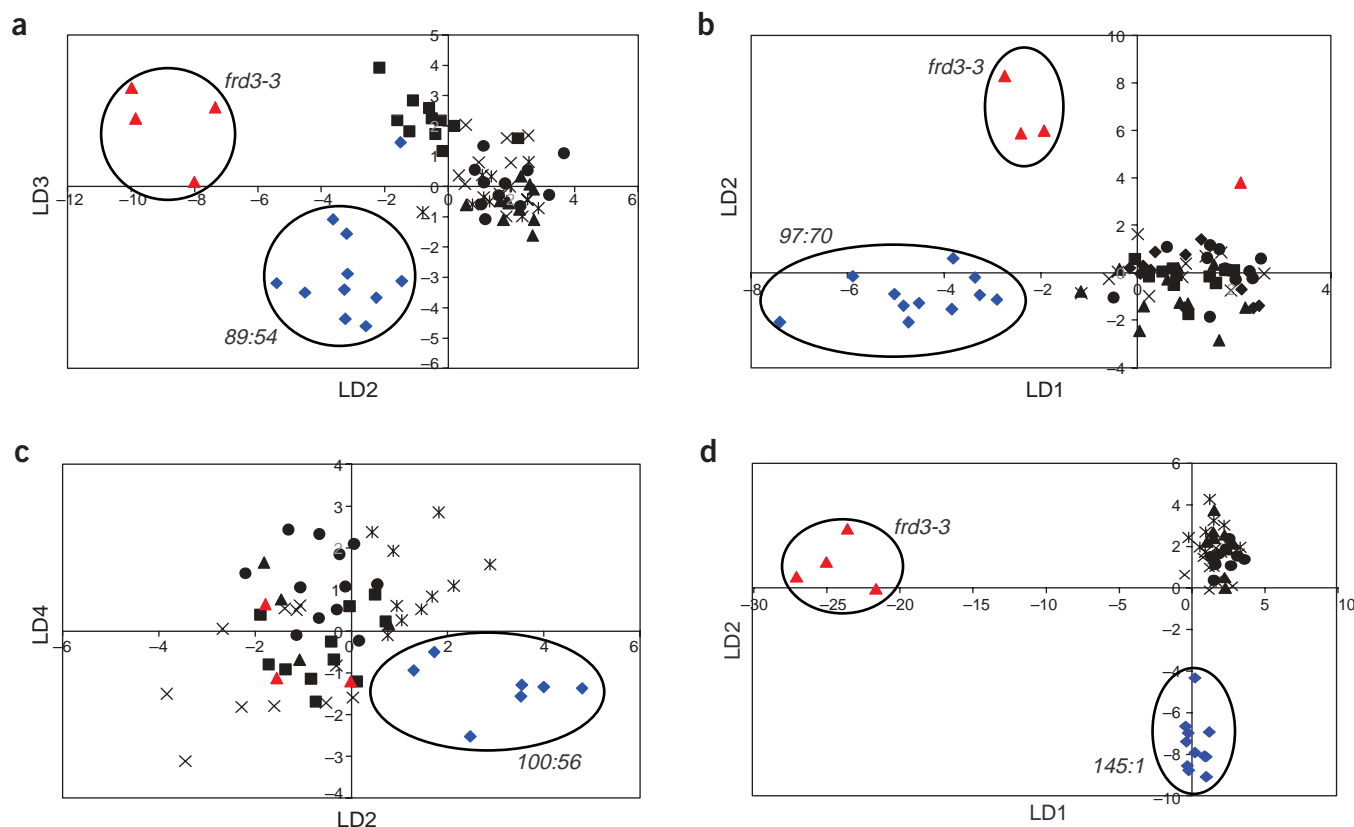


**Figure 4** Discriminant analysis of selected mutants. (a–d) Discriminant plots of four selected mutants 89:54 (a), 97:70 (b), 145:1 (c) and 100:56 (d), respectively, with each plot representing data from a separate M3 tray of plants. Red triangles represent *frd3-3*, blue diamonds the selected mutant, and black symbols wild-type and other putative M3 mutant lines in the tray of plants.

### Discriminant analysis resolves plants with altered profiles

Discriminant analysis is a statistical tool used for separation of groups in multidimensional space. Groups are separated by vectors (linear discriminants, LDs) representing a linear combination of the original data. The LDs are determined by maximizing the ratio of the difference between the means of the groups, scaled by the sample variance<sup>19</sup>. Discriminant analysis has been used widely, including in plant biochemistry<sup>20,21</sup>, molecular biology<sup>22</sup> and medicine<sup>23</sup>, to separate groups and has previously been applied in the separation of known mutant from wild-type plants<sup>24</sup>. Here we performed discriminant analysis on ICP-MS elemental profile data from all plants within a tray, where elemental profiles were considered as occupying 18-dimensional space, with each element representing a single dimension. Within the analysis, data were grouped into wild-type, *frd3-3* and the five M3 families under consideration in that tray. Separation of the groups was inspected visually by plotting the LDs against each other. LDs 1, 2 and 3 were found to routinely separate *frd3-3* from all other groups (Fig. 4a–c). Discriminant analysis also successfully separated M3 families (Fig. 4) previously designated as mutant (Figs. 1b and 2) using the four criteria outlined. Mutants 97:70 and 145:1 are clearly separated from the other M3 parental groups, wild-type and *frd3-3* by the first and second LDs (Fig. 4b,c). Mutant 89:54 is separated by the second and third LDs (Fig. 4a), and mutant 100:56 is separated by the second and fourth LDs (Fig. 4d). Discriminant analysis also showed that M3 plants from the remaining 40 mutants identified by ICP-MS (Table 1) were distinctly separated from all wild-type plants grown in the same tray. Discriminant analysis compares and separates mutants based on their

entire elemental profile, unlike the single-element comparisons used in *t*-test analyses. This different analytical approach makes discriminant analysis a robust and independent tool for confirmation of the mutant status of individual plant lines.

### DISCUSSION

Here we report data that establish the use of elemental profiling as a practical functional genomics tool for the identification of genes involved in the accumulation of mineral nutrients and trace elements in plants. We identified 44 confirmed *A. thaliana* mutants with altered shoot elemental profiles using ICP-MS and 7 using ICP-AES (Table 1). Within the mutant set identified by ICP-MS, a change in three elements was the most frequently observed mutant phenotype (Fig. 5a). Using ICP-MS we also identified changes in all 18 elements in our mutant population with varying frequencies (Fig. 5b). We also observed some interesting differences in the type of changes seen between the different elements (Fig. 5b). For example, the majority of mutants showing changes in calcium, iron or cobalt have lower concentrations than wild type, whereas most mutants showing changes in all other elements show higher concentrations. That only 11% of the mutants identified showed a change in the concentration a single element supports the idea that ion-homeostasis networks in plants are linked. This also further supports our contention that to achieve a full understanding of ion homeostasis in plants, it will be critical to uncover the underlying interaction networks that control the ionome.

Use of the mutant set described in this work for dissecting the genetic basis underlying the changes observed in the shoot ionome will require

positional cloning of genes of interest. Such cloning is based on the identification of plants with mutant phenotypes in the F2 inter-ecotype cross between mutant and wild type. For such a strategy to work, individual homozygous F2 mutant plants need to be reliably discriminated from the wild type based on changes in their ionome. An analysis of the ICP-MS data for mutants 71:13, 89:54, 97:70, 98:49, 100:56, 110:35, 112:50, 118:65, 145:01 and wild-type plants showed that of the 81 plants scored as mutant (altered by at least 2 s.d. in a single element from the mean wild type), only 2 were incorrectly scored as wild type, representing an error rate of 2.5% in mutant scoring. This would not be expected to significantly disturb the marker-assisted mapping of the gene of interest. This error rate would drop further if mutant scoring were based on changes in two or more elements. For mutants showing changes that are statistically less significant, confirmation of the mutant status of F2 plants from the inter-ecotype cross would require ICP-MS analysis of F3 families, increasing the analysis time required for mapping. Furthermore, it is important to consider that the phenotypes observed in the mutants described in this work occur under normal growth conditions, and the phenotypes may be amplified under special conditions. In support of this, the zinc- and arsenic-accumulating mutants 89:54 and 134:19 show enhanced sensitivity to these metals when the metals are present at elevated concentrations in the growth medium. If such visible phenotypes are found to cosegregate with the ionic phenotype, then F2 mutants could be visibly scored, markedly reducing the ICP-MS analysis time required for mapping.

For the positional cloning of genes of interest, it is also important that the ecotype chosen for crossing with the mutant not have an elemental profile significantly different from that of the parental line from which the mutant was derived. Because of the large number of unique genetic markers between the Col0 and Landsberg (Ler) ecotypes, Ler is the ecotype of choice for generation of F2 mapping populations. Elemental profile analysis of Ler reveals that this ecotype differs significantly from Col0 only in shoot concentrations of manganese, phosphorus and molybdenum, confirming that backcrossing to Ler can be used for mapping genes involved in alteration of at least 15 of the 18 elements analyzed.

The control of cellular and subcellular concentrations of nutrient elements, and the exclusion or compartmentalization of potentially toxic elements, require sensing elemental concentrations in the cytoplasm and extracellular space and within cellular compartments. Such information needs to be integrated and transduced to regulate appropriate transporters. Elemental profiling, as described here, will allow identification not only of transporters but also of sensors and other components that regulate expression and activity of the transport proteins. The identification in this screen of a mutation in *FRD3* (Fig. 3), a gene known to be involved in the regulation of iron acquisition from the soil<sup>14</sup>, also confirms the utility of this system for identifying genes involved in regulating interactions at the root-soil interface.

During the course of this work we have developed a robust system for performing a sustained analysis of large numbers of plants by ICP-MS. Although the analytical portion of the process is crucial, the statistical analyses of the data allow enhanced identification of mutants and scale up of these screens. Data handling and presentation also become a very large part of the overall project. Developing a workable data structure early on and adhering to it makes automation of the data-handling procedures much easier, increasing throughput and reducing errors. The high proportion of mutants identified with altered elemental profiles in the M1 fast neutron-mutagenized population (approximately 2%) suggests that numerous genes are involved in regulating mineral nutrient and trace element accumulation in *A. thaliana*. Assuming that all the mutants observed are independent, we can estimate that 2–4% of the

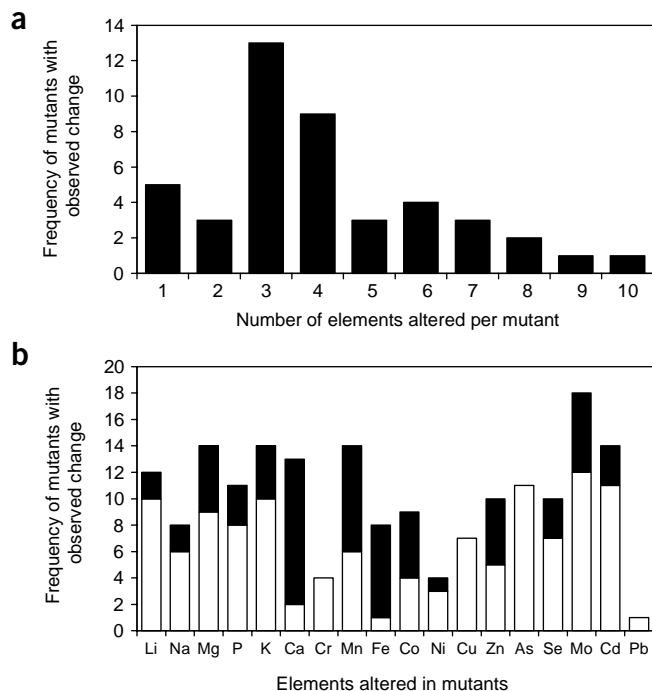


**Figure 5** Summary of the mutants identified by ICP-MS. (a) Frequency of mutants showing one or more changes in their elemental profile. (b) Frequency of mutants with increased (open bars) and decreased (solid bars) concentrations of a particular element.

genome of *A. thaliana* contributes to controlling the rosette leaf ionome of unstressed plants. However, further investigations of other tissues, including the root and seed, under various ionic challenges may well alter our early estimate of 2–4%. Furthermore, nutrient acquisition is likely to be mediated by control networks for which the rate-limiting genes are difficult to predict *a priori*. The random mutant screen developed here provides a useful approach for identifying critical elements in these networks in a higher eukaryote. Furthermore, the identified mutations could contribute to future strategies for engineering enhanced accumulation of nutrients and trace elements in plants.

## METHODS

**Plant culture at Purdue University.** Fast neutron-mutagenized M2 *A. thaliana* seeds (Lehle Seeds, M2F-02-01, Col0 parental group 4 and 6, progeny of the primary M1 mutagenized seeds) were planted using a Vacuseed (Polaris Instruments Ltd.), with three seeds planted per cell in 72-place grow-packs (26 cm × 52 cm). Plants were kept in a climate-controlled room at 19–24 °C with 8 h of light at 90–150 μE and were misted with 18 MΩ water daily. Seedlings were thinned after 1–2 weeks to leave a single plant closest to the middle of each cell and plants were sampled after 44 d. They were grown in Metro Mix 360 (Scotts) or Sunshine Mix no. 2 (Sun Gro Horticulture) with various elements added, including arsenic (As(v); 7.5 p.p.m.), cadmium (0.09 p.p.m.), cobalt (0.59 p.p.m.), chromium (Cr(vi); 0.26 p.p.m.), lithium (0.7 p.p.m.), sodium (4.7 p.p.m.), nickel (0.59 p.p.m.), lead (20 p.p.m.) and selenium (Se(vi); 7.9 p.p.m.), all subtoxic concentrations. Plants were bottom watered and fed with 0.1× or 0.25× Hoaglands solution at regular intervals. Plants were nondestructively sampled by removing two to three leaves (0.03–0.14 g fresh weight) and washing them with 0.1% Triton X-100 followed by 18 MΩ water before placing them in Pyrex digestion tubes. To induce flowering, individual plants were switched to 24-h light conditions.

**ICP-MS analysis at Purdue University.** In the primary screen M2 plants were analyzed in one of two ways. Plants in the first group, consisting of wild-type

Col0 plants (five per tray), were dried overnight at 92 °C and weighed before digestion. Those in the second group, consisting of the 60 mutant plants and 5 positive controls (*man1* (ref. 25), recently renamed *frd3-3* (ref. 14)) per tray, were dried and digested directly without weighing. Digestion was carried out in Pyrex tubes using 1.50 ml concentrated HNO<sub>3</sub> (Fisher TraceMetal grade) at 118 °C for 4 h. Each sample was diluted to 16.0 ml with 18 MΩ water and analyzed on a Thermo Elemental PQ ExCell ICP-MS using a glass conical nebulizer drawing 1 ml per min. Samples were run twice through the ICP-MS using both hot and cold plasma to measure 18 elements of interest. Beryllium, gallium and niobium internal standards (EM Science), National Institute of Standards and Technology traceable calibration standards (ULTRAScientific), and external drift correction were used. Analysis was performed by ICP-MS for lithium, sodium, magnesium, phosphorus, potassium, calcium, chromium, manganese, iron, cobalt, nickel, copper, zinc, arsenic, selenium, molybdenum, cadmium and lead, with later analyses replacing chromium with boron. To increase throughput, sample weights were derived from ICP-MS data by comparing the concentrations of potassium, calcium, manganese, copper, zinc, molybdenum and cadmium (elements quantified with the high precision and reliability) in the sample to those of weighed wild-type controls using the following calculation.

$$\frac{\text{Col0Signal}}{\text{WeightCol0}} \times \text{DilutionFactor} = \text{ConcentrationCol0} \quad (1)$$

$$\frac{\text{UnknownSignal}}{\text{WeightUnknown}} \times \text{DilutionFactor} = \text{ConcentrationUnknown} \quad (2)$$

$$\frac{\text{UnknownSignal}}{\text{ConcentrationCol0}} \times \text{DilutionFactor} = \text{WeightUnknown} \quad (3)$$

ConcentrationCol0 refers to the concentration of a given element in a Col0 *A. thaliana* sample, while ConcentrationUnknown refers to the concentration of that same element in a sample of a M2 or M3 fast neutron-mutagenized *A. thaliana* plant. The seven best weights for the unknown (derived from potassium, calcium, manganese, copper, zinc, molybdenum and cadmium) are averaged to yield the unknown's calculated weight. This calculation assumes that the ratio UnknownSignal/WeightUnknown is the same as the ratio Col0Signal/WeightCol0 (that is, the unknown has the same elemental profile as the Col0). This leads, after rearranging, to equation (3). After all weights are calculated, calculated weights that fail this assumption (perhaps as the result of a mutation) are omitted from the mean weight by discarding outliers in a three-iteration calculation (raw mean, far outliers omitted, near outliers omitted). These calculated weights were found to be linearly correlated with weights determined using a five-place balance over a 3.5-fold weight range with an  $R^2 = 0.89$ . Although this normalization technique was initially developed to increase sample throughput while still providing approximate dry weight concentrations, it was found that it allowed for less overall noise than did weighing every sample.

Once a plant was selected as a putative mutant, it was allowed to self-fertilize and replanted at  $n = 11$ . After 44 d of vegetative growth, before bolting, shoot material from M3 putative mutants was sampled and analyzed.

**Plant culture and ICP-AES-based analysis at the University of California San Diego.** Fast neutron-mutagenized *A. thaliana* seeds were planted in 28 mm × 55 mm trays, each tray containing 18 pots (90 mm × 90 mm), with an array 3 × 6, three seeds per pot. Plants were grown with 16 h light and stems and cauline leaves harvested after a drying period. Sample digestion was carried out in polypropylene tubes using <40 mg dry plant material per ml concentrated HNO<sub>3</sub> at 100 °C. Samples were diluted and run twice through an inductively coupled plasma atomic emission spectroscope (Vista, Varian) to measure 14 elements of interest. Yttrium was used as an internal standard. ICP-AES data were normalized to the corresponding weighed dry weights or in initial experiments to the magnesium concentration where indicated.

**Resources.** As part of this project we have released the complete elemental profiling data set described here to the public via a web-based, searchable database. Access to the database containing the ICP-MS data is available at the Salt laboratory website (<http://hort.agriculture.purdue.edu/Ionomics/database.asp>)

and access to the ICP-AES data is available at the Schroeder laboratory web site (<http://www-biology.ucsd.edu/labs/schroeder/supplemental.html>). Both data sets are also accessible through the PlantsT web site at <http://plantst.sdsc.edu/>. Along with the elemental profiling data, M3 seed from the 51 mutants identified from the ICP-MS and ICP-AES M2 screens has been submitted to the Arabidopsis Biological Resource Center ABRC (<http://www.biosci.ohio-state.edu/~plantbio/Facilities/abrc/abrchome.htm>) for distribution. Seed for all other lines screened in the M3 will be available on request from either the Salt or Schroeder laboratory collections, depending on the source of the mutant.

#### ACKNOWLEDGMENTS

This project is part of a larger collaborative effort funded by the National Science Foundation Plant Functional Genomics program (0077378-DBI) awarded to Mary Lou Guerinot, David Eide, Jeff Harper, David E. Salt and Julian Schroeder. More details about the collaborators and project can be found at <http://plantst.sdsc.edu/>. We also thank Venugopal Naga Venkata Gudimetla and Yanrong Zhaoy for assistance with database design and data analysis.

#### COMPETING INTERESTS STATEMENT

The authors declare that they have no competing financial interests.

Received 2 April; accepted 17 July 2003

Published online at <http://www.nature.com/naturebiotechnology/>

- Chory, J. *et al.* National Science Foundation-Sponsored Workshop Report: "The 2010 Project." Functional genomics and the virtual plant. A blueprint for understanding how plants are built and how to improve them. *Plant Physiol.* **123**, 423–425 (2000).
- Dangl, J. *et al.* The national plant genomics initiative: objectives for 2003–2008. *Plant Physiol.* **130**, 1741–1744 (2002).
- Aharoni, A. & Vorst, O. DNA microarrays for functional plant genomics. *Plant Mol. Biol.* **48**, 99–118 (2002).
- Finkelstein, D. *et al.* Microarray data quality analysis: lessons from the AFGC project. Arabidopsis Functional Genomics Consortium. *Plant Mol. Biol.* **48**, 119–131 (2002).
- Kerten, B. *et al.* Large-scale plant proteomics. *Plant Mol. Biol.* **48**, 133–141 (2002).
- Koller, A. *et al.* Proteomic survey of metabolic pathways in rice. *Proc. Natl. Acad. Sci. USA* **99**, 11969–11974 (2002).
- Fiehn, O. *et al.* Metabolite profiling for plant functional genomics. *Nat. Biotechnol.* **18**, 1157–1161 (2000).
- Roessner, U. *et al.* Metabolic profiling allows comprehensive phenotyping of genetically or environmentally modified plant systems. *Plant Cell* **13**, 11–29 (2001).
- Guerinot, M.L. & Salt, D.E. Fortified foods and phytoremediation: two sides of the same coin. *Plant Physiol.* **125**, 164–167 (2001).
- Daar, A.S. *et al.* Top ten biotechnologies for improving health in developing countries. *Nat. Genet.* **32**, 229–232 (2002).
- Mäser, P. *et al.* Phylogenetic relationships within cation-transporter families of *Arabidopsis thaliana*. *Plant Physiol.* **126**, 1646–1667 (2001).
- Outtern, C.E. & O'Halloran, T.V. Femtomolar sensitivity of metalloregulatory proteins controlling zinc homeostasis. *Science* **292**, 2488–2492 (2001).
- Williams, R.J.P. Chemical selection of elements by cells. *Coord. Chem. Rev.* **216**, 583–595 (2001).
- Rogers, E.E. & Guerinot, M.L. FRD3, a member of the multidrug and toxin efflux family, controls iron deficiency responses in *Arabidopsis*. *Plant Cell* **14**, 1787–1799 (2002).
- Li, X. & Zhang, Y. Reverse genetics by fast neutron mutagenesis in higher plants. *Funct. Integr. Genomics.* **2**, 254–258 (2002).
- Li, X. *et al.* A fast neutron deletion mutagenesis-based reverse genetic system for plants. *Plant J.* **27**, 235–242 (2001).
- Montgomery, D.C. *Introduction to Statistical Quality Control*, edn. 4 (Wiley, New York, 2001).
- Stadler, J.A. & Schweyen R.J. The yeast iron regulon is induced upon cobalt stress and crucial for cobalt tolerance. *J. Biol. Chem.* **277**, 39649–39654 (2002).
- Johnson, R.A. & Wichern, D.W. *Applied Multivariate Statistical Analysis*, edn. 3 (Prentice Hall, Englewood, New Jersey, 1992).
- Mannina, L. *et al.* Study of the cultivar-composition relationship in Sicilian olive oils by GC, NMR, and statistical methods. *J. Agric. Food Chem.* **51**, 120–127 (2003).
- Jakab, A. *et al.* Differentiation of vegetable oils by mass spectrometry combined with statistical analysis. *Rapid Commun. Mass Spectrom.* **16**, 2291–2297 (2002).
- Levitsky, V.G. & Katokhin, A.V. Recognition of eukaryotic promoters using a genetic algorithm based on iterative discriminant analysis. *In Silico Biol.* **3**, 0008 (2003).
- Leone, M., Larivière, G. & Comtois, A.S. Discriminant analysis of anthropometric and biomotor variables among elite adolescent female athletes in four sports. *J. Sports Sci.* **20**, 443–449 (2002).
- Vermerris, W. & Boon, J.J. Tissue-specific patterns of lignification are disrupted in the brown midrib2 mutant of maize (*Zea mays* L.). *J. Agric. Food Chem.* **49**, 721–728 (2001).
- Delhaize, E. A metal-accumulator mutant of *Arabidopsis thaliana*. *Plant Physiol.* **111**, 849–855 (1996).